Available online at www.sciencedirect.com
ScienceDirect
Journal of Organometallic Chemistry 692 (2007) 2365–2374
Journal of Organometallic Chemistry
www.elsevier.com/locate/jorganchem

Electrochemistry and complexation of Josiphos ligands

Brenna L. Ghent, Sarah L. Martinak, Lauren A. Sites, James A. Golen [1], Arnold L. Rheingold, Chip Nataro *

Department of Chemistry, Lafayette College, Easton, PA 18042, United States
Department of Chemistry and Biochemistry, University of California–San Diego, La Jolla, CA 92093, United States

Received 1 December 2006; received in revised form 7 February 2007; accepted 8 February 2007
Available online 6 March 2007

Abstract

The oxidative electrochemistry of 11 chiral bis-phosphinoferrocene ligands, all within the Josiphos class of ligands, was examined in methylene chloride. The oxidation of these ligands displays multiple waves of varying chemical reversibility. Palladium(II) and platinum(II) complexes with the general formula $[MCl_2(P–P)]$ (M = Pd or Pt; P–P = Josiphos) were prepared, characterized by NMR and cyclic voltammetry. The electrochemistry simplifies greatly upon coordination of the Josiphos ligands. The X-ray structures of a palladium(II) and platinum(II) complex of the same Josiphos ligand are reported.

Keywords: Electrochemistry; Cyclic voltammetry; Crystal structures; Josiphos ligands

1. Introduction

Asymmetric catalysis has become a growing field of study as the demand for more enantiomerically pure compounds arises. The major demand for these types of compounds is in the pharmaceutical industry because of the specificity needed for effective drugs [1]. Asymmetric catalysis requires that a chiral catalyst be used in order to transfer its chirality to the substrate. An effective asymmetric catalyst will quickly produce a chiral product in good yield with high enantiomeric purity of the desired enantiomer [2].

Compounds containing chiral metallocene ligands, in particular chiral ferrocenylphosphine ligands, are one class of asymmetric catalysts that has received significant attention in recent years due to the versatility of these catalysts in a variety of applications [3,4]. The ridged planar chirality enforced by the ferrocene backbone of ferrocenylphosphine is considered to be important to the effectiveness of the catalyst [3,4]. Typically, chiral ferrocenylphosphine ligands have a $–PR_2$ group bonded directly to one of the C_5 rings of the ferrocene and a chiral functional group bonded to the same C_5 ring but alpha to the $–PR_2$ group. The chiral group, typically a $–C^*HR^1R^2R^3$ group, can have various types of functional groups that change the electronic and/or steric properties of the ligand. It is thought that this functional group is what interacts with the reactants to force the formation of a chiral product [3,4]. A more recent development of the chiral ferrocenylphosphine ligands is a diphosphine ligand where the second phosphine is part of the chiral functional group that is bonded to the metallocene. An example of these types of ligands is Josiphos (Fig. 1). Josiphos ligands provide chiral catalysts that display two types of chirality, planar and central [5,6]. The two types of chirality have been found to be advantageous in a number of catalytic applications such as asymmetric allylic aminations and the asymmetric reduction of β-β-disubstituted enoates [5].

While complexes containing Josiphos ligands have proven to be effective in a number of catalytic applications the reasons why they are effective are not completely under-

* Corresponding author. Fax: +1 610 330 5714.
E-mail address: nataroc@lafayette.edu (C. Nataro).
[1] Permanent address: Department of Chemistry and Biochemistry, University of Massachusetts, Dartmouth, North Dartmouth, MA 02747, United States.

0022-328X/$ - see front matter © 2007 Elsevier B.V. All rights reserved.
doi:10.1016/j.jorganchem.2007.02.039

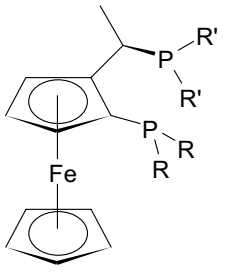

(**1**) R = Ph, R' = ^{t}Bu
(**2**) R = Cy, R' = ^{t}Bu
(**3**) R = 4-$C_6H_4CF_3$, R' = ^{t}Bu
(**4**) R = Cy, R' = Cy
(**5**) R = Ph, R' = Cy
(**6**) R = 3,5-Me_2-4-$OMeC_6H_2$, R' = Cy
(**7**) R = Ph, R' = 3,5-$C_6H_3Me_2$
(**8**) R = furanyl, R' = 3,5-$C_6H_3Me_2$
(**9**) R = 3,5-$C_6H_3(CF_3)_2$, R' = Cy
(**10**) R = 3,5-$C_6H_3(CF_3)_2$, R' = 3,5-$C_6H_3Me_2$
(**11**) R = Cy, R' = Ph

Fig. 1. Josiphos ligands.

stood. Several ideas as to the ligand characteristics that are the most important to the effectiveness of the catalyst have been proposed [3,4]. Unlike many other metallocene containing diphosphines, such as 1,1′-bis(diphenylphosphino)ferrocene (dppf), the phosphines of the Josiphos are attached to the same C_5 ring of the ferrocene backbone. The process by which they are synthesized is straightforward allowing for great variety in the types of R groups that can bonded to the phosphorus atoms [7,8]. Because of its versatility, these phosphines have been complexed with various metals and studied as catalysts in a variety of asymmetric reactions [2,5–41]. The varying R groups provide Josiphos complexes with a steric bulk that can be either a hindrance or an advantage. The steric hindrance of Josiphos was seen as an advantage in the palladium catalyzed amination of aryl tosylates due to the increase in the rate of the reaction, however, the reason for this increased rate is unknown [40]. In contrast, the catalytic hydrogenation of 3-alkylidenelactams using Josiphos containing catalysts gave very low yields and enantiomeric purity of the desired product due to the bulk of Josiphos [34].

While most of the work using Josiphos ligands has focused on catalytic properties, very little work has been done in terms of investigating the electronic nature of Josiphos ligands. This work reports the electrochemistry of 11 Josiphos ligands. The synthesis of the Pd(II) and Pt(II) dichloride complexes, which were characterized by NMR and cyclic voltammetry, is also reported. X-ray crystal structures were also obtained for a palladium and platinum complex and provide greater insight into the bonding of these ligands.

2. Experimental

2.1. General procedures

Standard Schlenk techniques under an argon atmosphere were used in the preparative reactions. Dichloromethane (CH_2Cl_2), diethyl ether (Et_2O), and hexanes were purified under Ar using a Solv-tek purification system similar to one previously described [42]. Acetonitrile (MeCN) was distilled over CaH_2 under Ar. NMR spectra were obtained in $CDCl_3$ using a JEOL Eclipse 400 FT-NMR. TMS ($\delta = 0.00$ ppm) was used as an internal standard for the ^{1}H NMR acquisitions. An external standard, 85% H_3PO_4, was used as the reference value for the $^{31}P\{^1H\}$ NMR data. Elemental analysis was performed by Quantitative Technologies, Inc. Ferrocene, decamethylferrocene and the Josiphos ligands were purchased from Strem. Ferrocene was purified by sublimation prior to use. Bis(benzonitrile)dichloropalladium(II) and *cis*-bis(acetonitrile)dichloroplatinum(II), were purchased from Aldrich. Compounds **1PdCl$_2$** [31], **2PdCl$_2$** [43], **5PdCl$_2$** [44], **9PdCl$_2$** [45] and **5PtCl$_2$** [46] were prepared according to literature procedures. Tetrabutylammonium hexafluorophosphate ($[NBu_4][PF_6]$) was purchased from Aldrich and dried *in vacuo* prior to use. Tetrabutylammonium tetrakis(pentafluorophenyl)borate ($[NBu_4][B(C_6F_5)_4]$) was metathesized from $Li[B(C_6F_5)_4]$ (Boulder Scientific Co.) according to the literature procedure [47].

2.2. Electrochemistry

All of the experiments were performed at ambient temperature (22 ± 1 °C) under an Ar atmosphere using 10.0 mL of a 0.1 M solution of $[NBu_4][PF_6]$ in CH_2Cl_2. The working electrode was a 1.5 mm glassy carbon electrode with a platinum wire as the auxiliary electrode and an Ag/AgCl (non-aqueous) reference electrode separated from the solution by a fine glass frit. The analyte concentration was 1.0 mM and the cyclic votammetric data was collected using a Princeton Applied Research 263-A potentiostat at scan rates of 100–1000 mV/s at 100 mV/s intervals. Depending on the potentials at which oxidation of the analyte occurred, either ferrocene or decamethylferrocene was added at the end of the experiment to give a solution that was 1.0 mM in the standard [48].

Using a CH Instruments Model 630B Electrochemical Analyzer, bulk electrolysis experiments were performed under an atmosphere of argon. Platinum mesh baskets were used as the working and auxiliary electrodes and the electrodes were placed in compartments separated by a fine glass frit. In the same compartment as the working electrode was the Ag/AgCl reference electrode, but it was also separated by a fine glass frit. Cyclic voltammograms were obtained before and after the bulk electrolysis using a 1.5 mm glassy carbon working electrode. Linear scan voltammograms were obtained with a 10 μm glassy carbon working electrode at scan rates of 10 and 25 mV/s before and after the bulk electrolysis. Experiments were conducted in CH_2Cl_2 using either 0.1 M $[NBu_4][PF_6]$ or 0.05 M $[NBu_4][B(C_6F_5)_4]$. The concentration of the analyte was 2.0 mM and the temperature was 22 ± 1 °C.

2.3. X-ray crystallography

Crystallographic data are contained in Table 1. Crystals of **2PdCl$_2$** and **2PtCl$_2$** were mounted on nylon loops. Laue symmetry and systematic absences in the data indicated a monoclinic setting for **2PdCl$_2$** and trigonal for **2PtCl$_2$**. In

Table 1
Crystal data and structure refinement for X-ray structures

	[**2PdCl$_2$**] · 0.67Et$_2$O	[**2PtCl$_2$**] · 0.67Et$_2$O
Formula	$C_{104}H_{176}Cl_6Fe_3O_2P_6Pd_3$	$C_{34.667}H_{58.667}Cl_2FeO_{0.667}P_2Pt$
Formula weight	2343.72	869.96
Crystal system	Monoclinic	Trigonal
Space group	$P2_1$	$P3_121$
a (Å)	18.1892(11)	15.1502(6)
b (Å)	16.8713(11)	151502(6)
c (Å)	19.3683(12)	27.332(2)
α (°)	90	90
β (°)	111.3910(10)	90
γ (°)	90	120
V (Å^3)	5534.2(6)	5432.9(5)
Z	2	6
D_{calc}	1.406	1.505
Crystal size (mm)	0.30 × 0.30 × 0.10	0.30 × 0.20 × 0.20
Crystal color	Orange	Orange
Temperature (K)	100(2)	100(2)
Radiation; λ (Å)	0.71073	0.71073
Absorption coefficient	1.137	4.513
F(000)	2448	2472
θ Range (°)	2.56–27.49	2.69–27.50
Data collected		
h	−23 to 23	−19 to 19
k	−21 to 21	−19 to 19
l	−25 to 24	−35 to 35
Number of data collected	49038	46487
Number of unique data	22065	7859
Absorption correction	SADABS	SADABS
Final R indices (obs. data)		
R_1	0.0375	0.0229
wR_2	0.0803	0.0543
Goodness-of-fit	1.048	1.095

both cases, chiral space groups were indicated and these choices were confirmed, along with the correct enantiomer, by refinement of the Flack parameter, which yielded values near zero for both. The structures were solved by direct methods and refined using anisotropic thermal parameters for the non-hydrogen atoms. Hydrogen atoms were idealized. In both cases, the asymmetric unit consists of a 3:2 ratio of complex to the recrystallization solvent, diethylether. For **2PtCl$_2$**, a model for the badly disordered solvent was created using SQUEEZE [49]; for **2PdCl$_2$**, the solvent was ordered and treated normally.

2.4. Synthesis

2.4.1. Palladium complexes

Equal molar amounts (approximately 0.05 mmol) of the desired Josiphos ligand and $(C_6H_5CH_2CN)_2PdCl_2$ were dissolved in 5.0 mL of CH_2Cl_2 and stirred for 24 h. The solution was then filtered using a cannula and the solvent was removed *in vacuo*. The solid was washed with three 5.0 mL portions of Et_2O and the resulting solid was dried *in vacuo*, yielding the desired complex. The colors of the compound, yields and $^{31}P\{^1H\}$ NMR data are presented in Table 2. The ^1H NMR and elemental analysis data for all new compounds are presented below. Crystals of **2PdCl$_2$** were prepared by dissolving the solid in 2.0 mL of CH_2Cl_2 and then layered the solution with 20.0 mL of Et_2O. The solution was left in the freezer for 5 days and a gel containing crystals of **2PdCl$_2$** formed. The gel was allowed to thaw; the solvent was decanted which yielded crystals suitable for X-ray analysis.

Compound **3PdCl$_2$**: ^1H NMR ($CDCl_3$): δ (ppm) 8.61 (m, 2H, –$C_6H_4CF_3$), 7.9–7.5 (m, 6H, –$C_6H_4CF_3$), 4.70 (br, s, 1H, C_5H_3), 4.50 (br, s, 1H, C_5H_3), 4.21 (m, 1H, C*H*Me), 3.97 (s, 5H, Cp), 3.89 (br, s, 1H, C_5H_3), 2.11 (dd, $^3J_{H-H}$ and $^3J_{H-P}$ = 10.1 and 7.1 Hz, 3H, C–CH_3), 1.64 (d, $^3J_{H-P}$ = 13.6 Hz, 9H, ^{t}Bu), 1.45 (d, $^3J_{H-P}$ = 15.0 Hz, 9H, ^{t}Bu). Anal. Calc. for $C_{34}H_{38}Cl_2F_6FeP_2Pd$: C, 47.72; H, 4.48. Found: C, 48.07; H, 4.34%.

Compound **4PdCl$_2$**: ^1H NMR ($CDCl_3$): δ (ppm) 4.84 (br, s, 1H, C_5H_3), 4.54 (br, s, 1H, C_5H_3), 4.51 (br, s, 1H, C*H*Me), 4.26 (s, 5H, Cp), 3.67 (br, s, 1H, C_5H_3), 2.33–0.77 (m, 47H, C–CH_3 and –Cy). Anal. Calc. for $C_{36}H_{56}Cl_2FeP_2Pd \cdot 0.25CH_2Cl_2$: C, 54.07; H, 7.07. Found: C, 54.30; H, 7.43%.

Compound **6PdCl$_2$**: ^1H NMR ($CDCl_3$): δ (ppm) 7.92 (d, $^3J_{H-P}$ = 12.8 Hz, 2H, –$C_6H_2Me_2OMe$); 7.17 (d, $^3J_{H-P}$ = 12.1 Hz, 2H, –$C_6H_2Me_2OMe$); 4.56 (br, s, 1H, C_5H_3), 4.36 (br, s, 1H, C_5H_3), 4.21 (br, s, 1H, C_5H_3), 3.79 (s, 3H, –OCH_3); 3.69 (s, 5H, Cp), 3.47 (m, 1H, C*H*Me), 2.39 (s, 6H, –CH_3), 2.21 (s, 6H, –CH_3), 1.8–1.2 (m, 22H, –Cy); 0.91 (m, 3H, C–CH_3). Anal. Calc. for $C_{42}H_{56}Cl_2FeO_2P_2Pd$: C, 56.81; H, 6.36. Found: C, 56.55; H, 6.39%.

Compound **7PdCl$_2$**: ^1H NMR ($CDCl_3$): δ (ppm) 8.1–7.0 (m, 16H, –C_6H_5 and –$C_6H_3Me_2$), 4.42 (s, 1H, C_5H_3), 4.36 (s, 1H, C_5H_3), 4.01 (s, 1H, C_5H_3), 3.64 (s, 5H, Cp), 3.61 (m, 1H, C*H*–Me), 2.42 (s, 6H, –CH_3), 2.18 (s, 6H, –CH_3), 1.00 (dd, $^3J_{H-H}$ and $^3J_{H-P}$ = 10.14 and 7.3 Hz, 3H, C–CH_3). Anal. Calc. for $C_{40}H_{40}Cl_2FeP_2Pd$: C, 58.89; H, 4.94. Found: C, 59.20; H, 5.02%.

Compound **8PdCl$_2$**: ^1H NMR ($CDCl_3$): δ (ppm) 7.9–7.2 (m, 6H, –$C_6H_3Me_2$); 7.01 (s, 2H, furanyl), 6.66 (m, 2H, furanyl), 6.56 (m, 2H, furanyl), 4.25 (br, 2H, C_5H_3), 4.09 (s, 1H, C_5H_3), 3.89 (s, 5H, Cp), 3.62 (m, 1H, C*H*Me), 2.41 (s, 6H, –CH_3), 2.22 (s, 6H, –CH_3), 1.17 (m, 3H, CH–CH_3). Anal. Calc. for $C_{36}H_{36}Cl_2FeO_2P_2Pd$: C, 54.33; H, 4.56. Found: C, 54.50; H, 4.73%.

Compound **10PdCl$_2$**: ^1H NMR ($CDCl_3$): δ (ppm) 8.5–7.0 (m, 12H, –$C_6H_3Me_2$ and –$C_6H_3(CF_3)_2$); 4.82 (br, s, 1H, C_5H_3), 4.58 (br, s, 1H, C_5H_3), 4.07 (br, s, 1H, C_5H_3), 3.82 (m, 1H, C*H*Me), 3.62 (s, 5H, Cp), 2.40 (s, 6H, –CH_3), 2.18 (s, 6H, –CH_3), 1.22 (m, 3H, C–CH_3). Anal. Calc. for $C_{44}H_{36}Cl_2F_{12}FeP_2Pd$: C, 48.58; H, 3.34. Found: C, 48.24; H, 3.58%.

Compound **11PdCl$_2$**: ^1H NMR ($CDCl_3$): δ (ppm) 7.8–7.3 (m, 10H, –C_6H_5); 4.70 (br, s, 1H, C_5H_3), 4.35 (br, s, 1H, C_5H_3), 4.23 (br, s, 1H, C_5H_3), 3.48 (s, 5H, Cp), 3.42 (m, 1H, C*H*Me), 2.4–1.1 (m, 25H, C–CH_3 and –Cy).

Table 2
Data for(**1–11**)**$PdCl_2$**

	$^{31}P\{^1H\}$ NMR data				% Yield	Color
	$^{31}P^a$	$^2J_{P-P}{}^b$	$^{31}P^a$	$^2J_{P-P}{}^b$		
3$PdCl_2$	24.8	s	113.4	s	32	Red
4$PdCl_2$	33.1	s	91.4	s	20	Light orange
6$PdCl_2$	80.9	6.94	20.7	6.94	50	Light brown
7$PdCl_2$	47.9	s	16.4	s	58	Yellow
8$PdCl_2$	60.3	s	−13.4	s	33	Orange
10$PdCl_2$	49.0	10.4	15.9	10.4	48	Red-brown
11$PdCl_2$	65.6	s	34.1	s	63	Orange

[a] In ppm.
[b] In Hz.

$C_{36}H_{44}Cl_2FeP_2Pd \cdot 0.5CH_2Cl_2$: C, 53.84; H, 5.57. Found: C, 53.67; H, 5.63%.

2.4.2. Platinum complexes

Equal molar amounts (approximately 0.05 mmol) of the desired Josiphos ligand and $(CH_3CN)_2PtCl_2$were dissolved in 5.0 mL of CH_2Cl_2 and stirred for 1 h. The solution was filtered via cannula and the volume was reduced to approximately 0.5 mL. Et_2O (10.0 mL) was then added causing the product to precipitate. The solution was filtered using a cannula and the solid was washed with three 5.0 mL portions of Et_2O. The remaining solid was dried *in vacuo*, yielding the desired complex. Data for the characterization of these platinum complexes is found in Table 3. The elemental analysis and ^1H NMR data for the new complexes are presented below. Crystals of **2$PtCl_2$** were prepared by dissolving the complex in approximately 0.5 mL of CH_2Cl_2 in a vial. The vial was then placed in a second vial containing Et_2O. The outer vial was capped and place in a refrigerator. The Et_2O slowly diffused into the CH_2Cl_2 solution over 5 days resulting in the formation of a gel. The gel was pierced with a needle and after 48 h crystals suitable for X-ray analysis formed.

Compound **1$PtCl_2$**: ^1H NMR ($CDCl_3$): δ (ppm) 8.48 (m, 2H, $-C_6H_5$), 7.6–7.3 (m, 8H, $-C_6H_5$), 4.60 (br, s, 1H, C_5H_3), 4.38 (br, s, 1H, C_5H_3), 3.97 (s, 5H, Cp), 3.85 (br, s, 1H, C_5H_3), 3.30 (m, 1H, C*H*Me), 2.08 (dd, $^3J_{H-H}$ and $^3J_{H-P} = 10.4$ and 7.1 Hz, 3H, C–CH_3), 1.58 (d, $^3J_{H-P} = 16.5$ Hz, 9H, ^{t}Bu), 1.41 (d, $^3J_{H-P} = 14.3$ Hz, 9H, ^{t}Bu). Anal. Calc. for $C_{32}H_{52}Cl_2FeP_2Pt$: C, 47.54; H, 4.99. Found: C, 47.91; H, 4.84%.

Compound **2$PtCl_2$**: ^1H NMR ($CDCl_3$): δ (ppm) 4.88 (br, s, 1H, C_5H_3), 4.54 (br, s, 1H, C_5H_3), 4.50 (br, s, 1H, C_5H_3), 4.28 (s, 5H, Cp), 3.88 (m, 1H, C*H*Me), 2.00 (dd, $^3J_{H-H}$ and $^3J_{H-P} = 10.4$ and 7.2 Hz, 3H, C–CH_3), 1.63 (d, $^3J_{H-P} = 13.2$ Hz, 9H, ^{t}Bu), 1.24 (d, $^3J_{H-P} = 14.3$ Hz, 9H, ^{t}Bu), 2.56–0.87 (m, 22H, –Cy). Anal. Calc. for $C_{32}H_{52}Cl_2FeP_2Pt$: C, 46.84; H, 6.39. Found: C, 46.62; H, 6.53%.

Compound **3$PtCl_2$**: ^1H NMR ($CDCl_3$): δ (ppm) 8.60 (m, 2H, $-C_6H_4CF_3$), 7.9–7.6 (m, 6H, $-C_6H_4CF_3$), 4.69 (br, s, 1H, C_5H_3), 4.47 (br, s, 1H, C_5H_3), 4.21 (m, 1H, C*H*Me), 3.97 (s, 5H, Cp), 3.85 (br, s, 1H, C_5H_3), 2.11 (dd, $^3J_{H-H}$ and $^3J_{H-P} = 10.2$ and 7.3 Hz, 3H, C–CH_3), 1.61 (d, $^3J_{H-P} = 12.8$ Hz, 9H, ^{t}Bu), 1.42 (d, $^3J_{H-P} = 14.6$ Hz, 9H, ^{t}Bu). Anal. Calc. for $C_{34}H_{38}Cl_2F_6FeP_2Pt \cdot 0.5CH_2Cl_2$: C, 41.99; H, 3.98. Found: C, 41.70; H, 3.63%.

Compound **4$PtCl_2$**: ^1H NMR ($CDCl_3$): δ (ppm) 4.80 (br, s, 1H, C_5H_3), 4.50 (br, s, 1H, C_5H_3), 4.45 (br, s, 1H, C*H*Me), 4.25 (s, 5H, Cp), 3.64 (br, s, 1H, C_5H_3), 2.3–0.8 (m, 47H, C–CH_3 and –Cy). Anal. Calc. for $C_{36}H_{56}Cl_2FeP_2Pt \cdot 0.25\ CH_2Cl_2$: C, 48.71; H, 6.37. Found: C, 48.34; H, 6.22%.

Table 3
Data for (**4-11**)**$PtCl_2$**

	$^{31}P\{^1H\}$ NMR data						% Yield	Color
	$^{31}P^a$	$^2J_{P-P}{}^b$	$^1J_{P-Pt}{}^b$	$^{31}P^a$	$^2J_{P-P}{}^b$	$^1J_{P-Pt}{}^b$		
1$PtCl_2$	76.7	13.9	3800	2.35	13.9	3600	37	Orange
2$PtCl_2$	75.8	13.8	3830	5.43	13.9	3530	37	Orange
3$PtCl_2$	77.1	17.3	3760	3.40	17.3	3630	20	Yellow-orange
4$PtCl_2$	54.6	s	3680	8.82	s	3520	69	Light orange
6$PtCl_2$	45.8	13.9	3580	−1.59	13.9	3600	62	Orange
7$PtCl_2$	24.5	24.3	3630	−2.71	24.3	3500	36	Light orange
8$PtCl_2$	32.1	20.7	3580	−32.4	20.8	3640	97	Dark yellow
9$PtCl_2$	46.3	17.3	3430	2.98	17.4	3570	77	Orange
10$PtCl_2$	25.2	17.3	3470	−0.37	17.3	3500	93	Light orange
11$PtCl_2$	38.3	17.3	3760	11.1	17.3	3410	60	Orange

[a] In ppm.
[b] In Hz.

Compound **6PtCl$_2$**: ^{1}H NMR ($CDCl_3$): δ (ppm) 7.90 (d, $^3J_{H-P} = 12.8$ Hz, 2H, –$C_6H_2Me_2OMe$); 7.15 (d, $^3J_{H-P} = 12.1$ Hz, 2H, –$C_6H_2Me_2OMe$); 4.53 (br, s, 1H, C_5H_3), 4.33 (br, s, 1H, C_5H_3), 4.18 (br, s, 1H, C_5H_3), 3.77 (s, 3H, –OCH_3); 3.54 (s, 5H, Cp), 3.45 (m, 1H, C*H*Me), 2.42 (s, 6H, –CH_3), 2.24 (s, 6H, –CH_3), 1.8–1.2 (m, 22H, –Cy); 0.94 (m, 3H, C–CH_3). Anal. Calc. for $C_{42}H_{56}Cl_2FeO_2P_2Pt$: C, 51.65; H, 5.78. Found: C, 51.51; H, 5.96%.

Compound **7PtCl$_2$**: ^{1}H NMR ($CDCl_3$): δ (ppm) 8.1–7.0 (m, 16H, –C_6H_5 and –$C_6H_3Me_2$), 4.37 (s, 1H, C_5H_3), 4.32 (s, 1H, C_5H_3), 3.97 (s, 1H, C_5H_3), 3.77 (m, 1H, C*H*–Me), 3.57 (s, 5H, Cp), 2.44 (s, 6H, –CH_3), 2.19 (s, 6H, –CH_3), 0.91 (m, 3H, C–CH_3). Anal. Calc. for $C_{40}H_{40}Cl_2FeP_2Pt$: C, 53.11; H, 4.46. Found: C, 52.90; H, 4.83%.

Compound **8PtCl$_2$**: ^{1}H NMR ($CDCl_3$): δ (ppm) 7.9–7.2 (m, 6H, –$C_6H_3Me_2$); 6.99 (s, 2H, furanyl), 6.63 (m, 2H, furanyl), 6.53 (m, 2H, furanyl), 4.24 (br, 2H, C_5H_3), 4.09 (s, 1H, C_5H_3), 3.75 (s, 5H, Cp), 3.62 (m, 1H, C*H*Me), 2.43 (s, 6H, –CH_3), 2.24 (s, 6H, –CH_3), 2.17 (m, 3H, CH–CH_3). Anal. Calc. for $C_{36}H_{36}Cl_2FeO_2P_2Pt$: C, 48.89; H, 4.10. Found: C, 48.75; H, 3.97%.

Compound **9PtCl$_2$**: ^{1}H NMR ($CDCl_3$): δ (ppm) 8.6–7.8 (m, 6H, –$C_6H_3(CF_3)_2$); 4.78 (br, s, 1H, C_5H_3), 4.53 (br, s, 1H, C_5H_3), 4.23 (br, s, 1H, C_5H_3), 3.63 (s, 5H, Cp), 3.47 (m, 1H, C*H*Me), 2.5–1.2 (m, 22H, –Cy), 0.87 (m, 3H, C–CH_3). Anal. Calc. for $C_{40}H_{40}Cl_2F_{12}FeP_2Pt \cdot 0.5CH_2Cl_2$: C, 41.40; H, 3.52. Found: C, 41.70; H, 3.63%.

Compound **10PtCl$_2$**: ^{1}H NMR ($CDCl_3$): δ (ppm) 8.5–7.0 (m, 12H, –$C_6H_3Me_2$ and –$C_6H_3(CF_3)_2$); 4.74 (br, s, 1H, C_5H_3), 4.54 (br, s, 1H, C_5H_3), 3.99 (br, s, 1H, C_5H_3), 3.82 (m, 1H, C*H*Me), 3.58 (s, 5H, Cp), 2.41 (s, 6H, –CH_3), 2.17 (s, 6H, –CH_3), 1.16 (m, 3H, C–CH_3). Anal. Calc. for $C_{36}H_{44}Cl_2FeP_2Pt$: C, 50.25; H, 5.15. Found: C, 50.13; H, 5.06%.

Compound **11PtCl$_2$**: ^{1}H NMR ($CDCl_3$): δ (ppm) 7.9–7.2 (m, 10H, –C_6H_5); 4.64 (br, s, 1H, C_5H_3), 4.31 (br, s, 1H, C_5H_3), 4.24 (br, s, 1H, C_5H_3), 4.23 (s, 5H, Cp), 3.47 (m, 1H, C*H*Me), 2.4–1.1 (m, 25H, C–CH_3 and –Cy). Anal. Calc. for $C_{44}H_{36}Cl_2F_{12}FeP_2Pt \cdot CH_2Cl_2$: C, 42.85; H, 3.04. Found: C, 42.70; H, 3.22%.

3. Results and discussion

The new complexes reported in this study were prepared using equal molar amounts of the desired Josiphos ligand and the appropriate MCl_2(nitrile)$_2$ (M = Pd or Pt). The reactions were performed in methylene chloride and the products precipitated upon addition of ether. The products were characterized by ^{1}H and ^{31}P{^{1}H} NMR. Since the phosphorus atoms are not equivalent, two peaks were observed in the ^{31}P{^{1}H} NMR. The $^2J_{P-P}$ coupling constants were typically in the range of 10–20 Hz, although in a number of the compounds, coupling was either not observed or unresolved. For the species containing platinum, the $^1J_{P-Pt}$ coupling constants were approximately 3500 Hz.

The oxidative electrochemistry of compounds **1**–**11** was investigated by cyclic voltammetry. Most of the Josiphos ligands displayed three oxidative waves (Table 4); the one at least positive potential is chemically and electrochemically irreversible, the intermediate wave displays varying amounts of chemical reversibility and the wave at the most positive potential is chemically and electrochemically reversible (Fig. 2). Ligands **2** and **4** display an additional wave that is partially chemically reversible. Ligands **2** and **4** are the only ligands that do not have aryl groups off either phosphine which may account for this additional wave. Ligands **9** and **10**, the only ligands that have 3,5-$C_6H_3(CF_3)_2$ groups, do not display the intermediate wave mentioned previously. There has been one previous report of the anodic electrochemistry of **11** in which three waves are noted, but the nature of these waves was not examined in detail [50].

Bulk anodic electrolysis, linear scan voltammetry (LSV) and cyclic voltammetry (CV) of **1** was performed in CH_2Cl_2 using either $[NBu_4][PF_6]$ or $[NBu_4][B(C_6F_5)_4]$ as

Table 4
Electrochemistry of Josiphos ligands and complexes in a solution of 0.1 M $[NBu_4][PF_6]$ in CH_2Cl_2

Compound	E_p^{ox} (V vs. $Fc^{0/+}$)	E_p^{ox} (V vs. $Fc^{0/+}$)	E_p^{ox} (V vs. $Fc^{0/+}$)	E^0 (V vs. $Fc^{0/+}$)
1	−0.01	0.33		0.47
1[a]	−0.02	0.43		0.56
1PdCl$_2$		0.35		
1PtCl$_2$		0.33		
2	−0.10	0.26	0.39	0.51
2PdCl$_2$		0.33		
2PtCl$_2$		0.31		
3	0.14	0.41		0.50
3PdCl$_2$		0.40		
3PtCl$_2$		0.41		
4	−0.12	0.25	0.42	0.68
4PdCl$_2$		0.33		
4PtCl$_2$		0.32		
5	0.03	0.34		0.46
5PdCl$_2$		0.43		
5PtCl$_2$		0.44		
6	0.01	0.32		0.45
6PdCl$_2$		0.30		
6PtCl$_2$		0.29		
7	0.10	0.31		0.47
7PdCl$_2$		0.33		
7PtCl$_2$		0.32		
8	0.08	0.31		0.47
8PdCl$_2$		0.30		
8PtCl$_2$		0.31		
9	0.25			0.47
9PdCl$_2$		0.48		
9PtCl$_2$		0.49		
10	0.27			0.45
10PdCl$_2$		0.51		
10PtCl$_2$		0.49		
11	0.00	0.44		0.65
11PdCl$_2$		0.33		
11PtCl$_2$		0.33		

[a] In a 0.05 M solution of $[NBu_4][B(C_6F_5)_4]$ in CH_2Cl_2.

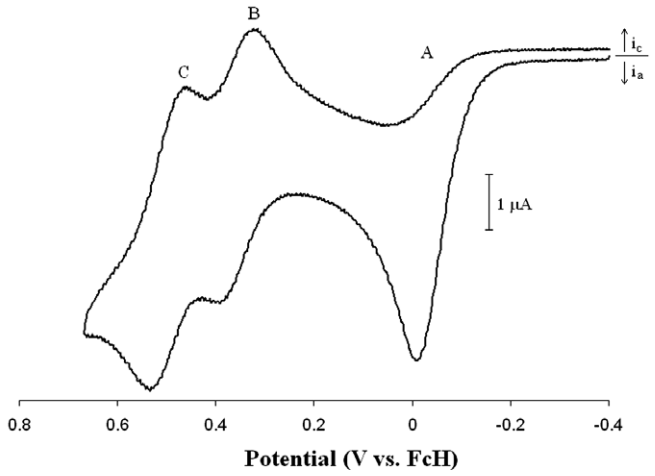

Fig. 2. Cyclic voltammetry scan of the oxidation of 1.0 mM **1** in CH_2Cl_2/0.10 M $[NBu_4][PF_6]$ at 100 mV/s.

the supporting electrolyte. Prior to bulk electrolysis, the LSV of **1** in solutions containing either supporting electrolyte displayed multiple features (Fig. 3). The diffusion coefficient of **1** was determined to be 1.9×10^{-5} in $[NBu_4][PF_6]$ and 2.1×10^{-5} in $[NBu_4][B(C_6F_5)_4]$. Bulk electrolysis at a potential positive of the wave labeled **A** (Fig. 2) gave one-electron transferred ($[NBu_4][PF_6]$: $n_{app} = 0.94\ e^-$, $E_{app} = 0.75$ V vs. Ag/AgCl based on a cyclic voltammogram of the bulk solution, $T = 22 + 1$ °C; $[NBu_4][B(C_6F_5)_4]$: $n_{app} = 0.96\ e^-$, $E_{app} = 1.15$ V vs. Ag/AgCl based on a cyclic voltammogram of the bulk solution, $T = 22 + 1$ °C). After the bulk electrolysis, the solution was examined by CV. Sweeping the potential positive of that used for the electrolysis showed the two waves at more positive potentials (Fig. 4) however no electroactive features were observed on the negative potential sweep. The oxidative LSV also displayed two features (Fig. 3) in the presence of either supporting electrolyte.

The second bulk electrolysis, for the wave marked **B** (Fig. 2), results in the transfer of one electron ($[NBu_4][PF_6]$: $n_{app} = 1.00\ e^-$, $E_{app} = 1.12$ V vs. Ag/AgCl based on a cyclic voltammogram of the bulk solution, $T = 22 + 1$ °C; $[NBu_4][B(C_6F_5)_4]$: $n_{app} = 0.98\ e^-$, $E_{app} = 1.54$ V vs. Ag/AgCl based on a cyclic voltammogram of the bulk solution, $T = 22 + 1$ °C). The CV and LSV after the second bulk oxidation in the presence of PF_6^- display one electroactive species which suggests that a reaction has occurred. The CV and LSV after the second oxidation in the presence of $B(C_6F_5)_4^-$ display two waves indicating the presence of two electroactive species (Fig. 3).

The wave marked **C** (Fig. 2) was a one-electron oxidation ($[NBu_4][PF_6]$: $n_{app} = 0.94\ e^-$, $E_{app} = 1.55$ V vs. Ag/AgCl based on a cyclic voltammogram of the bulk solution, $T = 22 + 1$ °C; $[NBu_4][B(C_6F_5)_4]$: $n_{app} = 0.98\ e^-$, $E_{app} = 1.80$ V vs. Ag/AgCl based on a cyclic voltammogram of the bulk solution, $T = 22 + 1$ °C). In PF_6^-, the LSV displays no electroactive species after the third bulk oxidation, while in $B(C_6F_5)_4^-$ there is one feature (Fig. 3). In addition, the CV in PF_6^- displays one reversible wave

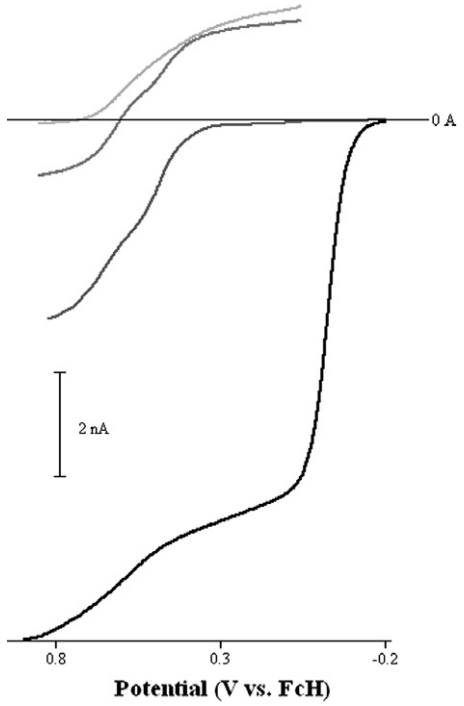

Fig. 3. Linear scan voltammery scans of the oxidation of 2.0 mM **1** in CH_2Cl_2/0.050 M $[NBu_4][B(C_6F_5)_4]$ at 25 mV/s prior to bulk electrolysis (—), after the first bulk electrolysis (—), after the second bulk electrolysis (—) and after the third bulk electrolysis (—).

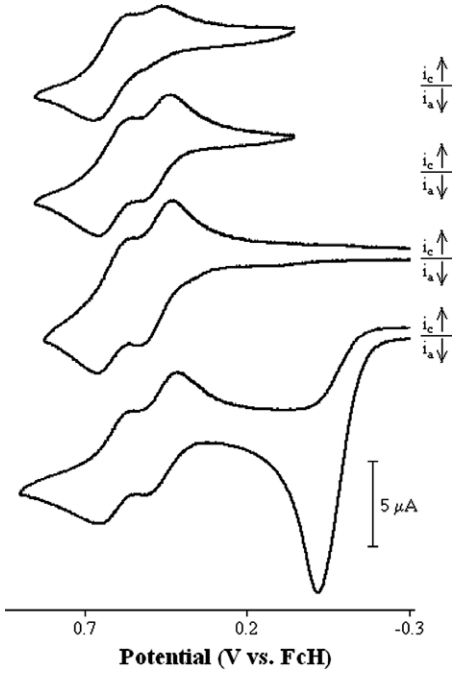

Fig. 4. Cyclic voltammery scans of the oxidation of 2.0 mM **1** in CH_2Cl_2/0.050 M $[NBu_4][B(C_6F_5)_4]$ at 100 mV/s prior to bulk electrolysis (bottom), after the first bulk electrolysis (second from bottom), after the second bulk electrolysis (second from top) and after the third bulk electrolysis (top).

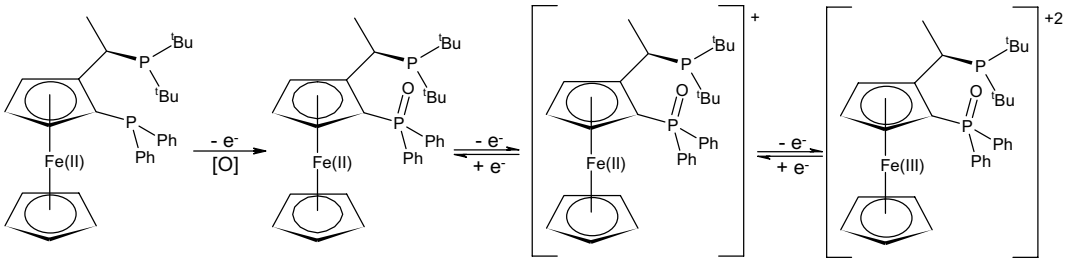

Scheme 1. Proposed mechanism for the oxidation of **1** on the CV timescale.

while the CV in $B(C_6F_5)_4^-$ displays a reversible wave and a chemically reversible wave (Fig. 4).

Oxidation of **1** in the presence of either supporting electrolyte likely follows an ECEE mechanism on the CV timescale (Scheme 1). The product after the first oxidation and chemical reaction is likely the phosphine oxide formed at the phosphorus bound to the C_5 ring. In comparing the potentials of **1**–**3**, the first wave (A) is very sensitive to the groups on the phosphorus bound directly to the C_5 ring, which also suggests that the initial oxidation occurs at that site. A $^{31}P\{^1H\}$ spectrum taken after the initial bulk electrolysis in either supporting electrolyte shows a small downfield shift (from 54 to approximately 50 ppm) for the $-P(tBu)_2$ group and a much more significant shift (from −25 to approximately 30 ppm) for the $-PPh_2$ group. The ^{31}P shift for the $-PPh_2$ group in **1** and the product of the first bulk electrolysis are reminiscent to those seen for dppf, −17 ppm [51,52], and the corresponding phosphine oxide, 1,1′-bis(diphenylphoshineoxide)ferrocene ($dppfO_2$), which occurs at 28.3 ppm [53].

The product of the second bulk electrolysis could not be isolated and the exact composition remains unknown. In solutions of either supporting electrolyte, the product of the oxidation appears to be stable on the CV time scale based on the reversibility of the wave. However, the solutions appear quite different after the bulk electrolysis; the color of the solution containing PF_6^- did not change significantly while the solution containing $B(C_6F_5)_4^-$ was yellow-green.

The NMR data suggests that on the bulk electrolysis time scale the product of the second oxidation is less stable in the presence of PF_6^- than $B(C_6F_5)_4^-$. The $^{31}P\{^1H\}$ spectrum of the bulk solution containing PF_6^- displayed a singlet at 51 ppm and a triplet (or overlapping doublet of doublets) at −15 ppm ($J = 974$ Hz). In the $^{31}P\{^1H\}$ spectrum of the solution containing $B(C_6F_5)_4^-$ there were two singlets, one at 62 ppm and the other at 47 ppm. Similar instability of oxidized species in the presence of PF_6^- but not $B(C_6F_5)_4^-$ have been noted for other systems [54,55]. The upfield shift of the peak in the ^{31}P NMR spectrum and the large coupling constant suggest that the phosphorus bound to the C_5 ring could be bonded to two fluorine atoms. The ^{31}P NMR spectrum of PPh_3F_2 shows a triplet at −56.1 ppm with a $^1J_{P-F}$ of 666 Hz [56]. The electrochemical preparation of R_3PF_2 compounds from $R_3P{=}O$ in the presence of HF has been reported [57]. We propose that the oxidation of the phosphine oxide is reversible on the CV time scale, however, in the presence of PF_6^- and on the bulk electrolysis time scale, the oxide is converted to a difluoride. Although $B(C_6F_5)_4^-$ is well known for its ability to stabilize highly reactive species [54,58], the CV in the presence of $B(C_6F_5)_4^-$ (Fig. 4) indicates chemical irreversibility of the second wave, suggesting that while more stable in the presence of this supporting electrolyte, the product of this oxidation will undergo a reaction. On the bulk electrolysis time scale, the oxidation of **1** likely follows an ECECE mechanism in which the second chemical step is dependent on the nature of the supporting electrolyte.

The product of the third bulk electrolysis was not isolated and its structure is unknown. In both cases, the color of the solution changed to green upon completing the third bulk oxidation. The $^{31}P\{^1H\}$ spectrum of the PF_6^- containing solution is identical to the spectrum after the second bulk electrolysis. The spectrum of the solution containing $B(C_6F_5)_4^-$ displays two singlets at 72 and 47 ppm. The significant color change and the small shift in the ^{31}P spectra suggest that the third oxidation occurs at the iron center. Further studies to isolate the oxidation products of these steps and investigate the low temperature stability of the oxidation products are underway.

The new $PdCl_2$ and $PtCl_2$ complexes of **1**–**4** and **6**–**11** were prepared by the reaction of the phosphines with the appropriate dichlorobisnitrile metal species. The products were characterized by NMR and, in general, the ^{31}P signals of the complexes were shifted downfield as compared to the free phosphines. In most of the compounds, phosphorus-phosphorus coupling was seen suggesting that both phosphorus atoms were bonded to the Pd(II) or Pt(II). For the $PtCl_2$ complexes, ^{195}Pt satellites were observed indicating that both phosphorus atoms are bonded directly to the Pt.

The structure of [**2PdCl$_2$**] (Fig. 5) was determined by X-ray diffraction. There are three distinct molecules of [**2PdCl$_2$**] in the unit cell; average bond lengths and angles for the three crystallographically independent molecules are presented in Table 5. The P_1–Pd distance is 0.036 Å longer than the P_2–Pd distance. In the asymmetric complexes, [**2PdBrPh**] and [**2PdIPh**], the differences were 0.131 and 0.1151 Å respectively; the difference in P–Pd bond lengths was attributes to the stronger *trans*-influence of phenyl as compared to the halide [29,43]. Somewhat surprisingly, the P–Pd distances are not significantly different

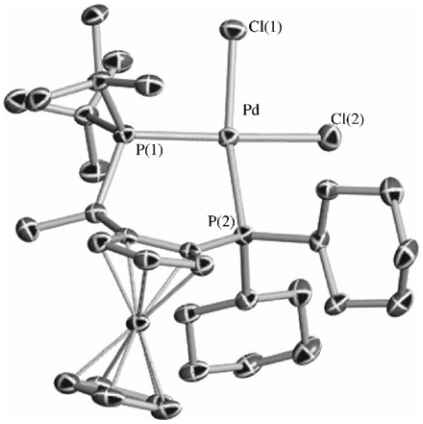

Fig. 5. ORTEP diagram of **2PdCl$_2$**.

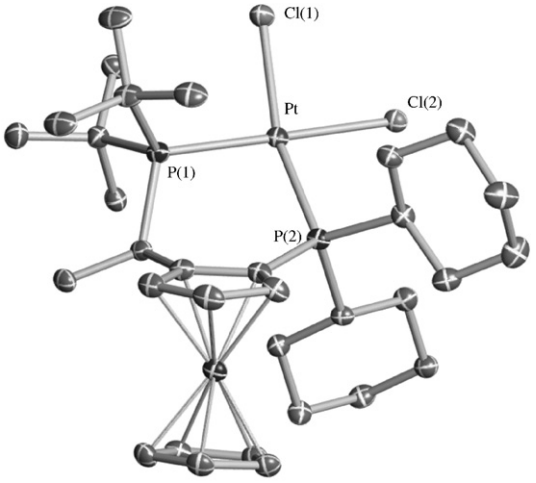

Fig. 6. ORTEP diagram of **2PtCl$_2$**.

Table 5
Average selected bond lengths (°) and distances (Å) for **2PdCl$_2$**

Bond lengths			
Pd–P_1	2.312	Pd–P_2	2.276
Pd–Cl_1	2.365	Pd–Cl_2	2.354
P_1–C_{chiral}	1.883	P_2–C_{Cp}	1.810
Avg. δ_P[a]	−0.306	Avg. δ_C[b]	−0.135
Bond angles			
P–Pd–P	97.03	Cl–Pd–Cl	86.48
P_1–Pd–Cl_1	92.41	P_2–Pd–Cl_2	87.74
P_1–Pd–Cl_2	167.88	P_2–Pd–Cl_1	160.53
X_a–Fe–X_b[c]	173.85	θ[d]	7.48

[a] Deviation of the P_2 atom from the C_5 plane, a positive value means the P_2 is closer to the Fe.
[b] Deviation of the C_{chiral} atom from the C_5 plane, a positive value means the P is closer to the Fe.
[c] Centroid–Fe–centroid.
[d] The dihedral angle between the two C_5 rings.

(0.00085 Å) in the related symmetric complex, [**2Pd(η^2-*trans*-stilbene)**] [43]. The geometry about the palladium can be described as distorted square planar. The P–Pd–P angle is greater than 90° while the Cl–Pd–Cl angle is less than 90° and the average angle between the planes defined by P_1–Pd–P_2 and Cl_1–Pd–Cl_2 is 21.23°. The P–Pd–P bite angle in [**2PdCl$_2$**] is approximately 1° smaller than that of [**2PdBrPh**] which is the smallest bite angle of **2** previously reported [29]. Looking down the P_1–C_{chiral} bond, the Me group on the chiral carbon is *anti*- to the palladium.

The structure of [**2PtCl$_2$**] was also determined, making it the second structure of a platinum Josiphos complex reported (Fig. 6). The P–Pt bond lengths in [**2PtCl$_2$**] are approximately 0.03 Å longer than the P–Pt distances in the other reported Josiphos platinum structure, [**5PtCl$_2$**] [47]. In addition, the P–Pt–P bite angle in [**2PtCl$_2$**] is approximately 2° larger than that found for the analogous complex with **5**. These differences are likely due to the more sterically demanding *tert*-butyl groups in **2**.

The structures of [**2PdCl$_2$**] and [**2PtCl$_2$**] provide the first opportunity to compare one Josiphos ligand bound to two different Group 10 metals that have the same ancillary ligands, in this case chloride. The P–Pt–P bite angle is slightly larger than the corresponding angle in the palladium analogue (Table 6). A similar trend has been noted in Pd(dppf)Cl_2 and Pt(dppf)Cl_2 [59,60]. As in the palladium analogue, the platinum in **2PtCl$_2$** is distorted from square planar geometry (Fig. 6). The angle between P_1–Pt–P_2 plane and the Cl_1–Pt–Cl_2 plane is 14.92°, which is significantly less than that found for the palladium analogue. In addition, the Me group of the stereocenter is pointing away from the platinum atom.

The oxidative electrochemistry of the Josiphos ligands simplified upon coordination to either Pd or Pt; only one chemically and electrochemically reversible oxidation was present (Fig. 7). Bulk anodic electrolysis confirmed that the oxidation of **1PdCl$_2$** and **1PtCl$_2$** are one-electron processes. For **1PdCl$_2$** the color changed from red to green-yellow upon oxidation ($n_{app} = 1.0$ e$^-$, $E_{app} = 1.05$ V vs. Ag/AgCl based on a cyclic voltammogram of the bulk solution, $T = 22 \pm 1$ °C) while **2PtCl$_2$** changed from yellow-orange

Table 6
Average selected bond lengths (°) and distances (Å) for **2PtCl$_2$**

Bond lengths			
Pt–P_1	2.2632(9)	Pt–P_2	2.2870(10)
Pt–Cl_1	2.3696(9)	Pt–Cl_2	2.3674(9)
P_1–C_{chiral}	1.886(4)	P_2–C_{Cp}	1.813(4)
δ_P[a]	−0.337	Avg. δ_C[b]	−0.069
Bond angles			
P–Pt–P	97.33(3)	Cl–Pt–Cl	83.54(3)
P_1–Pt–Cl_1	96.95(3)	P_2–Pt–Cl_2	93.80(3)
P_1–Pt–Cl_2	163.30(3)	P_2–Pt–Cl_1	172.11(3)
X_a–Fe–X_b[c]	173.56	θ[d]	7.97

[a] Deviation of the P_2 atom from the C_5 plane, a positive value means the P_2 is closer to the Fe.
[b] Deviation of the C_{chiral} atom from the C_5 plane, a positive value means the P is closer to the Fe.
[c] Centroid–Fe–centroid.
[d] The dihedral angle between the two C_5 rings.

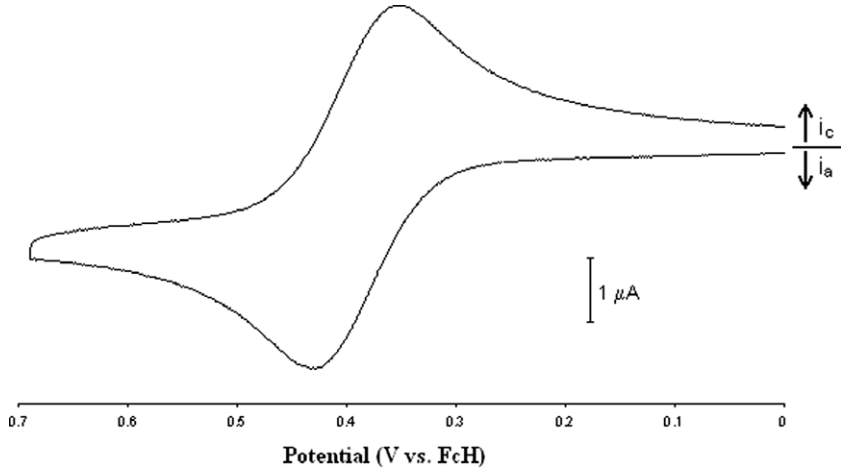

Fig. 7. Cyclic voltammetric scan of the oxidation of 1.0 mM **1PdCl$_2$** in CH_2Cl_2/0.10 M $[NBu_4][PF_6]$ at 100 mV/s.

to green ($n_{app} = 1.0$ e$^-$, $E_{app} = 1.00$ V vs. Ag/AgCl based on a cyclic voltammogram of the bulk solution, $T = 22 \pm 1$ °C). The potentials at which oxidation of the palladium complexes occur are within 0.02 V of the analogous platinum complexes. The potentials are sensitive to changing the groups on the Josiphos ligands, in particular the groups on the phosphorus bound directly to the C_5 ring; comparing the complexes of ligands **4**, **5**, and **11** provides the best example of this. The potentials at which oxidation of the palladium and platinum complexes of **4** and **11**, in which the only difference is cyclohexyl groups at the phosphorus off the chiral carbon, **4**, vs. phenyl, **11** are quite similar. However, there is an approximately 0.1 V difference between complexes of **4**, in which the change is cyclohexyl groups on the phosphorus bound to the C_5 rings, vs. complexes **5**, in which there are phenyl groups. The anticipated effect of electron withdrawing fluorinated-groups making the potential at which oxidation occurs more positive can be seen by comparing complexes of **1** vs. **3**, **5** vs. **9**, and **7** vs. **10**.

4. Summary

The oxidative electrochemistry of Josiphos ligands is complicated, displaying multiple waves in the CV. The oxidation is proposed to follow an ECEE mechanism on the CV timescale. The first oxidation is followed by a fast chemical reaction leading to the formation of the corresponding phosphine oxide. Evidence from the ^{31}P NMR indicates that the phosphine oxide forms on the phosphorus bound directly to the C_5 ring. The electrochemical process at the intermediate potential is likely due to oxidation of the phosphine oxide, possibly at a phenyl ring [61]. The final wave is likely due to oxidation of the iron center. Upon coordination to Pd(II) and Pt(II), the oxidative electrochemistry of Josiphos ligands simplify, giving rise to one reversible wave. The potentials at which oxidation of the Josiphos containing compounds occur are sensitive to the varying R groups. The structures of **2PdCl$_2$** and **2PtCl$_2$** were determined and the palladium and platinum atoms are distorted from square-planar geometry.

Acknowledgments

B.L.G., S.L.M., L.A.S., and C.N. thank the donors of the Petroleum Research Fund, administered by the American Chemical Society, for partial funding of this research, the Kresge Foundation for the purchase of the JEOL NMR and the Academic Research Committee at Lafayette College for funding EXCEL scholars. C.N. thanks Professor R.J. LeSuer of Chicago State University for helpful discussion in preparing this manuscript.

Appendix A. Supplementary material

CCDC 627003 and 627004 contain the supplementary crystallographic data for **2PdCl$_2$** and **2PtCl$_2$**. These data can be obtained free of charge via http://www.ccdc.cam.ac.uk/conts/retrieving.html, or from the Cambridge Crystallographic Data Centre, 12 Union Road, Cambridge CB2 1EZ, UK; fax: (+44) 1223-336-033; or e-mail: deposit@ccdc.cam.ac.uk. Supplementary data associated with this article can be found, in the online version, at doi:10.1016/j.jorganchem.2007.02.039.

References

[1] M. Butters, D. Catterick, A. Craig, A. Curzons, D. Dale, A. Gillmore, S.P. Green, I. Marziano, J.-P. Sherlock, W. White, Chem. Rev. 106 (2006) 3002.
[2] H.-U. Blaser, W. Breiden, B. Pugin, F. Spindler, M. Studer, A. Togni, Top. Catal. 19 (2002) 3, and references therein.
[3] K.-S. Gan, T.S.A. Hor, in: A. Togni, T. Hayashi (Eds.), Ferrocenes from Homogeneous Catalysis to Material Science, VCH, New York, 1995, p. 105.
[4] T.J. Colacot, Chem. Rev. 103 (2003) 3101.
[5] D.B. Berkowitz, G. Maiti, Org. Lett. 6 (2004) 2661.
[6] M. Lautens, K. Fagnou, Proc. Natl. Acad. Sci. U.S.A. 101 (2004) 5455.

[7] A. Togni, C. Breutel, A. Schnyder, F. Spindler, H. Landert, A. Tijani, J. Am. Chem. Soc. 116 (1994) 4062.
[8] B.H. Lipshutz, K. Noson, W. Chrisman, A. Lower, J. Am. Chem. Soc. 125 (2003) 8779.
[9] M.E.P. Lormann, M. Nieger, S. Braese, J. Organomet. Chem. 691 (2006) 2159.
[10] W. Xu, L.-B. Han, Org. Lett. 8 (2006) 2099.
[11] B.H. Lipshutz, N. Tanaka, B.R. Taft, C.-T. Lee, Org. Lett. 8 (2006) 1963.
[12] K. Makino, T. Fujii, Y. Hamada, Tetrahedron: Asymmetry 17 (2006) 481.
[13] J. Deschamp, O. Chuzel, J. Hannedouche, O. Riant, Angew. Chem., Int. Ed. 45 (2006) 1292.
[14] M. Kubryk, K.B. Hansen, Tetrahedron: Asymmetry 17 (2006) 205.
[15] M.A. Fernandez-Rodriguez, Q. Shen, J.F. Hartwig, J. Am. Chem. Soc. 128 (2006) 2180.
[16] L. Wu, J.F. Hartwig, J. Am. Chem. Soc. 127 (2005) 15824.
[17] M.E. Limmert, A.H. Roy, J.F. Hartwig, J. Org. Chem. 70 (2005) 9364.
[18] S.I. Pereira, J. Adrio, A.M.S. Silva, J.C. Carretero, J. Org. Chem. 70 (2005) 10175.
[19] K.B. Hansen, T. Rosner, M. Kubryk, P.G. Dormer, J.D. Armstrong III, Org. Lett. 7 (2005) 4935.
[20] C.S. Schultz, S.D. Dreher, N. Ikemoto, J.M. Williams, E.J.J. Grabowski, S.W. Krska, Y. Sun, P.G. Dormer, L. DiMichele, Org. Lett. 7 (2005) 3405.
[21] F. Lopez, S.R. Harutyunyan, A. Meetsma, A.J. Minnaard, B.L. Feringa, Angew. Chem., Int. Ed. 44 (2005) 2752.
[22] I.N. Houpis, L.E. Patterson, C.A. Alt, J.R. Rizzo, T.Y. Zhang, M. Haurez, Org. Lett. 7 (2005) 1947.
[23] W.P. Hems, P. McMorn, S. Riddel, S. Watson, F.E. Hancock, G.J. Hutchings, Org. Biomol. Chem. 3 (2005) 1547.
[24] Q. Shen, S. Shekhar, J.P. Stambuli, J.F. Hartwig, Angew. Chem., Int. Ed. 44 (2005) 1371.
[25] W. Baratta, E. Hertweck, K. Siega, M. Toniutti, P. Rigo, Organometallics 24 (2005) 1660.
[26] M.P. Muñoz, J. Adrio, J.C. Carretero, A.M. Echavarren, Organometallics 24 (2005) 1293.
[27] A. Leitner, J. Larsen, C. Steffens, J.F. Hartwig, J. Org. Chem. 69 (2004) 7552.
[28] Y. Hsiao, N.R. Rivera, T. Rosner, S.W. Krska, E. Njolito, F. Wang, Y. Sun, J.D. Armstrong III, E.J.J. Grabowski, R.D. Tillyer, F. Spindler, C. Malan, J. Am. Chem. Soc. 126 (2004) 9918.
[29] A.H. Roy, J.F. Hartwig, Organometallics 23 (2004) 194.
[30] B. Lipshutz, J.M. Servesko, B.R. Taft, J. Am. Chem. Soc. 126 (2004) 8352.
[31] A.H. Roy, J.F. Hartwig, J. Am. Chem. Soc. 125 (2003) 8704.
[32] B. Lipshutz, J.M. Servesko, Angew. Chem., Int. Ed. 42 (2003) 4789.
[33] R. Kadyrov, T.H. Riermeier, U. Dingerdissen, V. Tararov, A. Boerner, J. Am. Chem. Soc. 68 (2003) 4067.
[34] T. Yue, W.A. Nugent, J. Am. Chem. Soc. 124 (2002) 13692.
[35] M. Lautens, K. Fagnou, V. Zunic, Org. Lett. 4 (2002) 3465.
[36] M. Lautens, K. Fagnou, J. Am. Chem. Soc. 123 (2001) 7170.
[37] C. Larksarp, O. Sellier, H. Alper, J. Org. Chem. 66 (2001) 3502.
[38] M. Lautens, K. Fagnou, T. Rovis, J. Am. Chem. Soc. 122 (2000) 5650.
[39] M. Lautens, K. Fagnou, M. Taylor, Org. Lett. 2 (2000) 1677.
[40] B.C. Hamann, J.F. Hartwig, J. Am. Chem. Soc. 120 (1998) 7369.
[41] N.C. Zanetti, F. Spindler, J. Spencer, A. Togni, G. Rihs, Organometallics 15 (1996) 860.
[42] A.B. Pangborn, M.A. Giardello, R.H. Grubbs, R.K. Rosen, F.J. Timmers, Organometallics 15 (1996) 1518.
[43] T.J. Brunker, N.F. Blank, J.R. Moncarz, C. Scriban, B.J. Anderson, D.S. Glueck, L.N. Zakharov, J.A. Golen, R.D. Sommer, C.D. Incarvito, A.L. Rheingold, Oranometallics 24 (2005) 2730.
[44] M. Sperrle, G. Consiglio, J. Am. Chem. Soc. 117 (1995) 12130.
[45] C. Gambs, G. Consiglio, A. Togni, Helv. Chim. Acta 84 (2001) 3105.
[46] A. Togni, C. Breutel, M.C. Soares, N. Zanetti, T. Gerfin, V. Gramlich, F. Spindler, G. Rihs, Inorg. Chim. Acta 222 (1994) 3205.
[47] R. LeSuer, W.E. Geiger, Angew. Chem., Int. Ed. 39 (2000) 248.
[48] The value for ΔE^0 of Fc^* vs. FcH (V) for the conditions used in this study is −0.548 V. F. Barrière, W.E. Geiger, J. Am. Chem. Soc. 128 (2006) 3980.
[49] P. Van der Sluis, A.L. Spek, Acta Crystallogr., Sect. A 46 (1990) 194.
[50] S.R. Harutyunyan, F. López, W.R. Browne, A. Correa, D. Peña, R. Badorrrey, A. Meetsma, A.J. Minnaard, B.L. Feringa, J. Am. Chem. Soc. 128 (2006) 9103.
[51] A.L. Bandini, G. Banditelli, M.A. Cinellu, G. Sanna, G. Minghetti, F. Demartin, M. Manassero, Inorg. Chem. 28 (1989) 404.
[52] B. Corrain, B. Longato, G. Favero, D. Ajò, G. Pilloni, U. Russo, F.R. Kreissl, Inorg. Chim. Acta 157 (1989) 259.
[53] T.S.A. Hor, H.S.O. Chan, K.-L. Tan, L.-T. Phang, Y.K. Yan, L.-K. Liu, Y.-S. Wen, Polyhedron 10 (1991) 2437.
[54] N. Camire, A. Nafady, W.E. Geiger, J. Am. Chem. Soc. 124 (2002) 7260.
[55] F. Barriere, R.U. Kirss, W.E. Geiger, Organometallics 24 (2005) 48.
[56] W.J. Marshall, V.V. Grushin, Organometallics 22 (2003) 555.
[57] V.Ya. Semenii, V.A. Stepanov, N.V. Ignat'ev, G.G. Furin, L.M. Yagupol'skii, Zh. Obshch. Khim. 55 (1985) 2716.
[58] S. Trupia, A. Nafady, W.E. Geiger, Inorg. Chem. 42 (2003) 5480.
[59] I.R. Butler, W.R. Cullen, T.-J. Kim, S.J. Rettig, J. Trotter, Organometallics 4 (1985) 972.
[60] G.M. de Lima, C.A.L. Filgueiras, M.T.S. Giotto, Y.P. Mascarenhas, Transition Met. Chem. 20 (1995) 380.
[61] M.C.R. Symons, R. Janes, J. Chem. Soc.: Faraday Trans. 1 83 (1987) 383.